Drugs in R&D (2024) 24:425–434
https://doi.org/10.1007/s40268-024-00483-5

ORIGINAL RESEARCH ARTICLE

Preclinical and Toxicology Assessment of ALW-II-41-27, an Inhibitor of the Eph Receptor A2 (EphA2)

Theodore J. Kottom[1] · Kimberly E. Stelzig[1] · Madeline R. Pellegrino[1] · Marc Bindzus[1] · Eunhee S. Yi[2] · Andrew H. Limper[1]

Accepted: 28 July 2024 / Published online: 6 August 2024

Abstract

Background and Objective The EphA2 receptor inhibitor ALW-II-41-27 has proven to be an effective in vitro antagonist of *Pneumocystis* β-glucan-induced proinflammatory signaling. This suggests its potential as a candidate for initial anti-inflammatory drug testing in the rodent model of Pneumocystis pneumonia (PCP).

Methods Initially, single-dose intraperitoneal (IP) injections of ALW-II-41-27 were administered at concentrations of 0, 10, 15, 20, and 30 mg/kg over a 24-h treatment period. Pharmacokinetics were assessed in plasma, bronchoalveolar lavage fluid (BALF), and epithelial lining fluid (ELF). Following these assessments, a final single mg/kg dosing was determined. Mice received daily IP injections of either vehicle or 20.0 mg/kg of ALW-II-41-27 for 10 days, with their weights recorded daily. On day 11, mice were weighed and euthanized. Lungs, liver, and kidneys were harvested for H&E staining and pathology scoring. Lung samples were further analyzed for proinflammatory cytokines using enzyme-linked immunosorbent assay (ELISA) and extracellular matrix production using quantitative PCR (qPCR). Postmortem blood collection was conducted for complete blood count (CBC) blood chemistry analysis. Lastly, ALW-II-41-27 was administered to mice prior to fungal β-glucans challenge to determine in vivo effects on lung inflammation.

Results This report describes the PK assessment of ALW-II-41-27 given via IP in C57BL/6 mice. After PK data were generated, we tested ALW-II-41-27 at 20 mg/kg IP in mice and noted no significant changes in daily or final weight gain. ELISA results of proinflammatory cytokines from lung tissues showed no major differences in the respective groups. qPCR analysis of extracellular matrix transcripts were statistically similar. Examination and pathology scoring of H&E slides from lung, liver, and kidney in all groups and subsequent pathology scoring showed no significant toxicity. Blood chemistry and CBC analyses revealed no major abnormalities. Additionally, administering ALW-II-41-27 before intratracheal inoculation of fungal β-glucans, known to induce a strong proinflammatory response in the lungs, significantly reduced lung tissue IL-1β levels.

Conclusions In our initial general safety and toxicology assessments, ALW-II-41-27 displayed no inherent safety concerns in the analyzed parameters. These data support broader in vivo testing of the inhibitor as a timed adjunct therapy to the deleterious proinflammatory host immune response often associated with anti-*Pneumocystis* therapy.

Key Points

An inhibitor of the EphA2 receptor termed ALW-II-41-27 was well tolerated when administered via intraperitoneal (IP) injection to mice.

Administration of ALW-II-41-27 prior to intratracheal (IT) administration of yeast β-glucans resulted in significant reductions in the host inflammatory response.

✉ Theodore J. Kottom
kottom.theodore@mayo.edu

[1] Thoracic Diseases Research Unit, Departments of Medicine and Biochemistry, Mayo Clinic, 8-23 Stabile, Rochester, MN 55905, USA

[2] Department of Laboratory Medicine and Pathology, Mayo Clinic, Rochester, MN 55905, USA

1 Introduction

Eph receptor A2 (EphA2) is a transmembrane receptor and part of the tyrosine kinase (RTK) receptor family. This receptor has important roles in cancer, aberrant angiogenesis, and inflammation associated with atherosclerosis. More recently, this receptor pathway has also emerged as an important regulatory pathway for host defense against microbial pathogens, including bacterial, viral, and fungal pathogens [1–5]. For instance, in oropharyngeal candidiasis, EphA2 receptor was shown to be a receptor for fungal β-glucans in oral epithelial cells and linked to proinflammatory signaling via signal transducer and activator of transcription 3 (STAT3) and mitogen-activated protein kinase (MAPK) [6]. Furthermore, our laboratory has recently shown that in mouse lung epithelial cells, the EphA2 receptor is also involved in binding *Pneumocystis* and that β-glucans from the organism can activate downstream signaling through EphA2 engagement, leading to release of lung epithelial IL-6 release [7]. We have also recently published that a small molecule inhibitor of the EphA2 receptor, termed ALW-II-41-27, can dampen in vitro macrophage immune proinflammatory response to *Pneumocystis* β-glucans [8]. These data provide initial proof of concept that timed intervention of ALW-II-41-27 during or after anti-*Pneumocystis* treatment may greatly improve the deleterious effects on the host caused by organism killing and release of proinflammatory carbohydrates [9]. This study was conducted to evaluate the short-term administration of EphA2 inhibitor ALW-II-41-27 in mice via IP administration and examine potential detrimental responses to the inhibitor through tissue, inflammatory, and toxicological analyses. Lastly, we present data that ALW-II-41-27 can significantly dampen fungal induced lung inflammation after β-glucan challenge in the lung. The data shown here demonstrate the safety of ALW-II-41-27 and endorse its wider clinical development as an EphA2 inhibitor for in vitro use in the animal models. In. addition, these data support its further development as a therapeutic option to manage Pneumocystis pneumonia (PCP)-related inflammation during anti-*Pneumocystis* treatment.

2 Methods

2.1 Animals

Male and female C57BL/6 mice at 7–12 weeks of age were used for experiments. Mice underwent a mandatory 2-day acclimation period at the Mayo Clinic before any experiments can be performed. The mice were separated by gender and housed four to five to a cage. The mice were fed PicoLab Mouse Diet 20 5058* ad libitum and watered from an automatic watering valve. Included in the housing the mice were provided "standard enrichment material" for the facility of two Twist-n'Rich and a Bed-r'Nest (The Andersons Plant Nutrient Group). All animal procedures were performed in accordance with the Laboratory Animal Welfare Act, the Guide for the Care and Use of Laboratory Animals Welfare Act, and the Mayo Clinic Institutional Animal Care and Use Committee (IACUC) (approval number: A00005722-20).

2.2 Administration of ALW-II-41-27

ALW-II-41-27 was obtained for Sigma-Aldrich. Dose selection (20 mg/kg) was based on pharmacokinetic (PK) data described below. Due to the lack of solubility of the inhibitor in water or saline, the inhibitor was prepared first by dissolving the compound in 100% dimethyl sulfoxide (DMSO), followed by the addition of 0.5% Methocel in 0.9% NaCl for injection at a 10%/90% vol/vol ratio. Intraperitoneal (IP) treatment (100 µl) with the DMSO/Methocel (vehicle, control mice group) or the 20 mg/kg of ALW-II-41-27 inhibitor in DMSO/Methocel was initiated on day 0 and subsequentially every day for 10 days. At day 11, mice were sacrificed, and subsequent analyses performed as described.

2.3 Pharmacokinetic Analysis

Single-dose PK experiments were conducted in mice to assess concentrations over time in the plasma and epithelial lining fluid (ELF) of the lung. ALW-II-41-27 was administered to immunocompetent uninfected female C57BL/6 by the intraperitoneal (IP) route, followed by blood sampling at eight terminal time points with cardiac puncture at 0.25, 0.5, 1, 2, 4, 6, 8, and 24 h postdosing. Bronchoalveolar lavage fluid (BALF) was also collected at termination. Plasma and BALF were analyzed by liquid chromatography–tandem mass spectrometry (LC–MS/MS). Urea concentrations in BALF and plasma served as the endogenous marker of the ELF [10] dilution for calculation of the analyte ELF concentrations. The pharmacokinetic parameters for each dose level were obtained from the noncompartmental analysis (NCA) of the plasma and ELF concentration data using WinNonlin: $t_{1/2}$, T_{max}, C_{max}, AUC_{last}, AUC_{Inf}, AUC/D, AUCExtr, MRT, Vz_F, and CL_F. The ratios of ELF concentrations over time relative to plasma were calculated and plotted.

2.4 ELISA determination of Cytokine Release

Cytokines were analyzed from total lung homogenates using enzyme-linked immunosorbent assay (ELISA) kits to measure mouse IL-1β, IL-6, and TNFα that were purchased from Thermo Fisher Scientific [11].

2.5 Quantitative Polymerase Chain Reaction Analysis

To extract RNA from mouse lung, tissue was lysed and homogenized with Buffer RLT Plus (supplied with the RNeasy Plus Mini Kit; Qiagen). The lysate was passed through a genomic DNA eliminator spin column, ethanol was added, and the samples were applied to a RNeasy MinElute spin column according to the manufacturer's instructions. An iScript Select cDNA synthesis kit (Bio-Rad, Hercules, CA) was used for reverse transcription employing oligo (dT) primers and random hexamer primer mix. A SYBR green PCR kit (Bio-Rad) was used for quantitative real-time PCR and was performed and analyzed on a CFX96 Touch Real-Time PCR Detection System (Bio-Rad) [11]. The sequences of the primer pairs are listed in Supplementary Table 1.

2.6 Biochemical Analysis

For blood chemistry analysis, serum was analyzed with the Piccolo Xpress Chemistry Analyzer according to the manufacturer's instructions [11]. For the veterinary hematology [complete blood count (CBC)] assay, an Abaxis VetScan HM5 Analyzer was used [12].

2.7 Histology Analysis

For histological analysis, lung, liver, and kidney samples were fixed in 10% neutral formalin. Paraffin embedding and staining were performed at the Mayo Clinic Histology Core, Scottsdale, AZ. Sections (5 μm) were stained with H&E and graded blindly for the extent of organ inflammation by a Mayo Pathologist (ESY). The sections were scored as follows: 1+, mild perivascular aggregates; 2+, heavy perivascular aggregates; 3+, mild alveolar aggregates; 4+, alveolar exudate and heavy alveolar aggregates; and 0, normal. These scores were based upon grading of the entire organ surface area present on the slide section [11].

2.8 In Vivo Inflammatory Analysis of ALW-II-41-27

To determine whether administration of ALW-II-41-27 via IP injection might result in systemic distribution and inhibitory effects on the host lung inflammatory response, the following experiment was conducted. Briefly, 20 h prior to giving mice 100 μg/ml *Saccharomyces cerevisiae* β-glucans via intratracheal (IT) injection (similar to [11]), mice were given 0.1 mg/kg ALW-II-41-27 or the vehicle control via intraperitoneal as noted. The next day at 18 h post-ALW-II-41-27 or vehicle treatment, mice were given another 0.1 mg/kg of ALW-II-41-27, or vehicle as stated. After 2 h, mice were given ±100 μg/ml *S. cerevisiae* β-glucans (Sigma-Aldrich) via IT. The following day mice were sacrificed, and lung protein lysates measured for IL-1β.

2.9 Statistical Analysis

For multigroup data, the initial analysis was first performed with analysis of variance (ANOVA) to determine overall different differences. If ANOVA indicated overall differences, subsequent group analysis was then performed by a two-sample unpaired Student *t* test for normally distributed variables. For the PK studies, sample sizes of 24 mice per group for each dosing (mg/kg) were used. For the 10-day IP injections of 20 mg/kg of ALW-II-41-27, a sample size of eight was used, and equal amounts of male and female mice were used for each group. Based on our earlier mouse studies, we estimate that there was a power of at least 0.9 to detect a difference for a given parameter representing 1.5 times within-group standard deviation. Since there were no discernable differences in the data based upon gender, the data from all mice were combined for the reported results. For the in vivo studies analyzing the effects of ALW-II-41-27 on β-glucans-induced lung inflammation, the samples size for each group was 11–12 mice. Evaluation of data was conducted using Prism 9 for macOS, version 10.2.3 (GraphPad, San Diego, CA). Values of $p < 0.05$ were considered significant.

3 Results

3.1 Pharmacokinetics

3.1.1 Plasma PK for ALW-II-41-27

The concentration–time profile of ALW-II-41-27 in plasma following IP administrations of ALW-II-41-27 is shown in Fig. 1A using the information tabulated in Supplementary Table 2. The PK parameters, including $t_{1/2}$, T_{max}, C_{max}, AUC_{last}, AUC_{Inf}, AUC/D, AUCExtr, MRT, Vz_F and CL_F, are provided in Supplementary Table 3 and were calculated using noncompartmental analysis (NCA) with WinNonlin. All time points with measurable concentrations were used for the NCA analysis. ALW-II-41-27 at 10, 15, 20, and 30 mg/kg IP, yielded plasma C_{max} and AUC_{last} parameters that correlated linearly with dose across the concentration range with R^2 values of 0.7729 and 0.9970, respectively

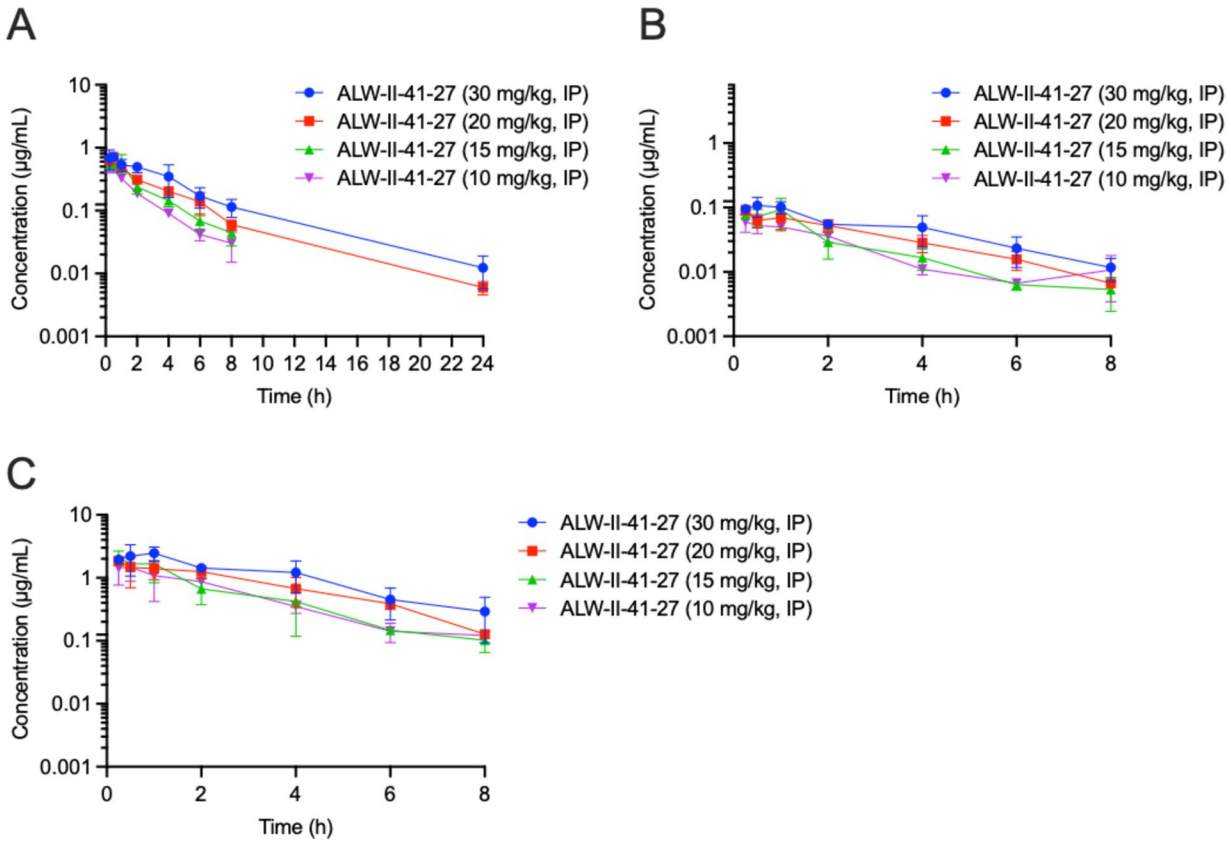

Fig. 1. The mean plasma (**A**), BALF (**B**), and ELF (**C**) concentration–time profiles of ALW-II-41-27 IP single administration to uninfected C57BL/6 mice. Error bars are SD values

(Supplementary Figs. 1 and 2). The respective plasma C_{max} values ranged from 0.488 to 0.716 µg/ml and the AUC_{last} values ranged from 1.123 to 2.738 h µg/ml (Supplementary Table 4).

3.1.2 ELF PK for ALW-II-41-27

The concentration–time profile of ALW-II-41-27 in ELF following IP administrations of ALW-II-41-27 is plotted in Fig. 1C using the information tabulated in Supplementary Table 2. The PK parameters, including $t_{1/2}$, T_{max}, C_{max}, AUC_{last}, AUC_{Inf}, AUC/D, AUCExtr, MRT, Vz_F and CL_F, are provided in Supplementary Table 5 and were calculated using all time points with measurable concentrations, noncompartmental analysis with WinNonlin. ALW-II-41-27 at 10, 15, 20, and 30 mg/kg IP, yielded ELF C_{max} and AUC_{last} parameters that correlated linearly with dose with R^2 values of 0.7478 and 0.9779, respectively (Supplementary Figs. 1 and 2). The C_{max} values ranged from 1.489 to 2.468 µg/ml and the AUC_{last} values ranged from 4.141 to 8.928 h µg/ml (Supplementary Table 5). The ELF penetration values (AUC_{last} ELF/AUC_{last} plasma) ranged from 291% to 369% with the tested doses of 10, 15, 20, and 30 mg/kg IP (Fig. 1C). Based on the results of the plasma and ELF data, for the 10-day daily single administration of ALW-II-41-27 a dose of 20 mg/kg was used.

3.2 ALW-II-41-27 IP Administration Resulted in no Significant Weight Loss

Administration of ALW-II-41-27 at 20.0 mg/kg IP results in no significant changes in daily and ending weight loss (Fig. 2).

3.3 Measurements of Lung Cytokines in ALW-II-41-27 IP Administration and Control Groups

The production of the inflammatory cytokine IL-1β, IL-6, and TNF-α were measured in whole-lung lysates and are shown in Fig. 3A–C**.** No significant alterations were noted from the vehicle control.

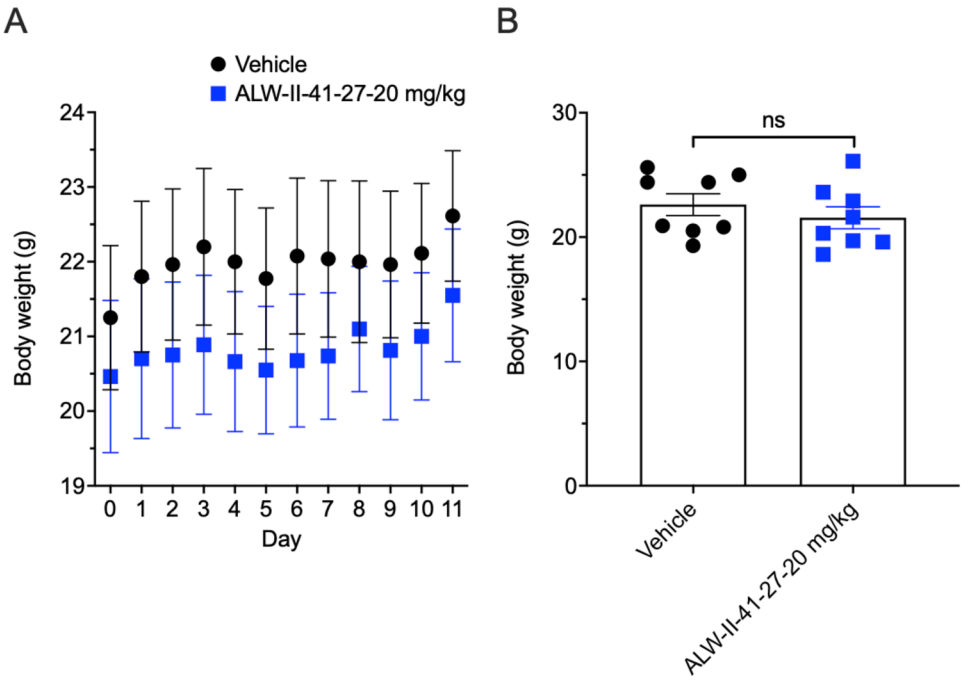

Fig. 2. Effects of mouse body weight with IP administration daily of ALW-II-41-27. **A** Shows the daily weight changes in the vehicle control versus the 20.0 mg/kg doses of IP administered ALW-II-41-27 daily for 10 days. **B** Shows the final weights for the two groups after 11 days. ($n = 8$ mice/group). No significant weight changes were noted between the two groups

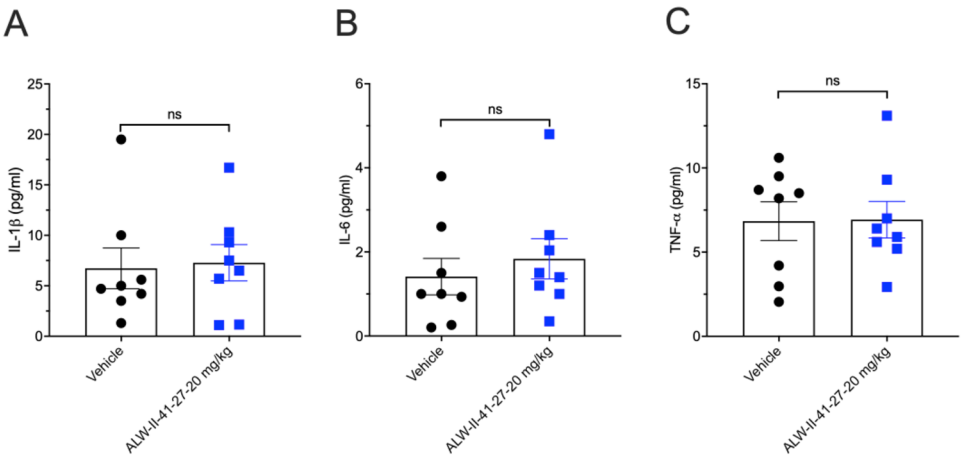

Fig. 3. EphA2 inhibitor ALW-II-41-27 effects on lung proinflammatory cytokine production. **A** IL-1β, **B** IL-6, and **C** TNF-α production was measured from total lung lysates from day 11 of the experiment. ($n = 8$ mice/group). No significant differences were noted between the groups

3.4 Analysis of mRNA Extracellular Matrix Generation

qPCR was implemented to determine the levels of mRNA expression of Collagen Type Alpha 1 Chain (*Col1a1*) and Fibronectin (*Fn*), both extracellular matrix-related genes used as markers for profibrotic development [13]. Beta 2 microglobulin (*B2M*) was used as a housekeeping gene. As shown in (Fig. 4A, B), no significant differences were noted in the two groups at day 11 in the respective lung samples.

3.5 Serum Chemistry Data

Complete group mean serum chemistry data from day 11 are shown in Fig. 5A–J. Between both treatment groups, there were no significant changes except for creatinine (CRE) levels, which were significantly lower in the ALW-II-41-27 treatment cohort, although this parameter was not clinically significant and was within the normal published range for mice [14]. The mechanisms for the reduction of creatinine in the treated group are unknown but may be related to somewhat lower dietary intake and reduced muscle mass over the course of the treatment, although this was not reflected in a significant difference in body weight (Fig. 2B).

3.6 Complete Blood Count (CBC) Data

CBC data from day 11 are shown in Fig. 6A–L. There were no significant differences between any the ALW-II-41-27

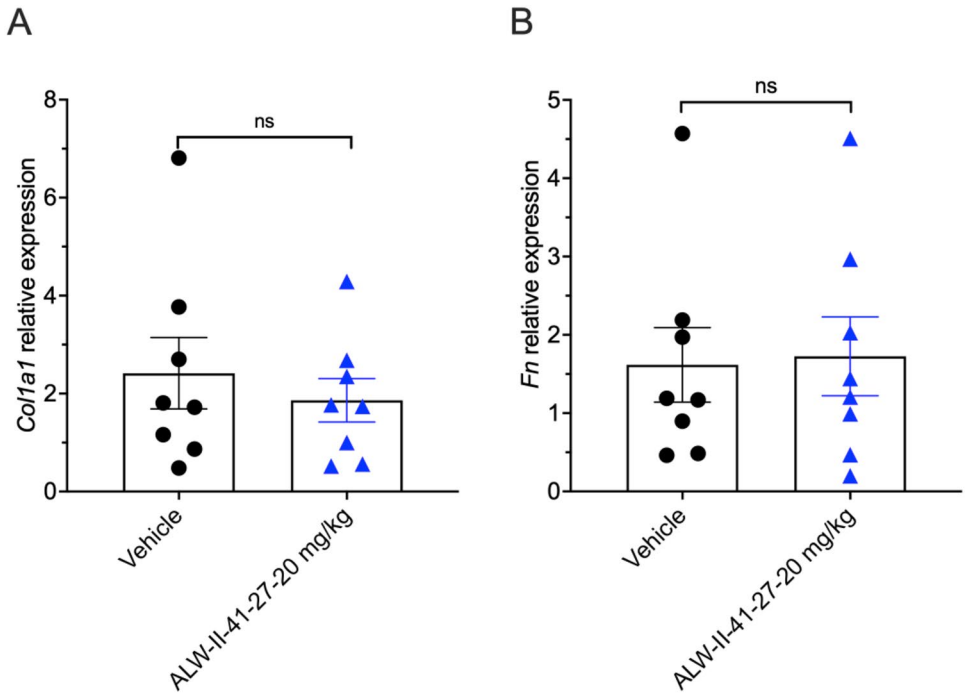

Fig. 4. Quantitation of *Col1a1* and *Fn* mRNA in total lung RNA after vehicle and ALW-II-41-27 administration for 10 days. Ratios of **A** *Col1a1* and **B** *Fn* to *B2M* in total lung RNA. ($n = 8$ mice/group). No significant differences were noted between the groups

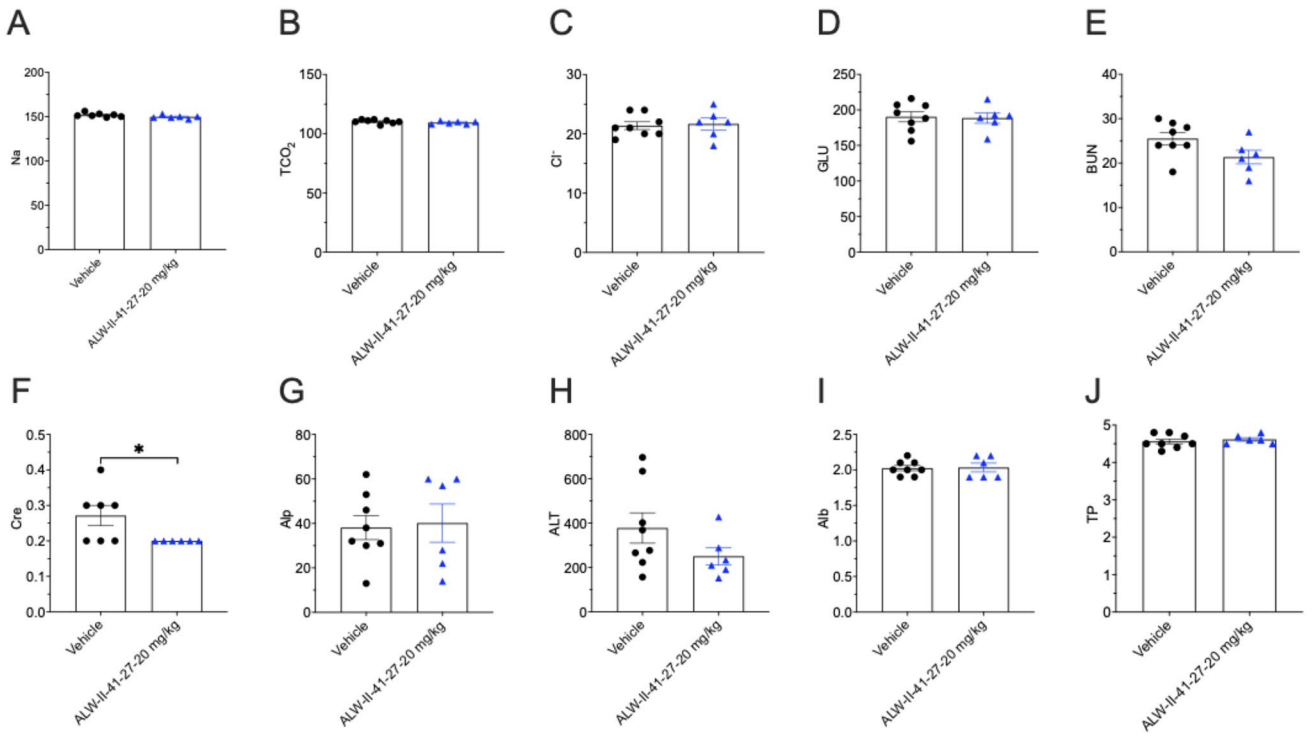

Fig. 5 Serum chemistry parameters. Na, sodium (mmol/l); tCO_2 (mmol/l); carbon dioxide (mmol/l); Cl, chloride (mmol/l); GLU, glucose (mg/dl); BUN, blood urea nitrogen (mg/dl); Cre, creatine (mg/dl); Alp, alkaline phosphatase (U/L); ALT, alanine aminotransferase (U/L); Alb, albumin (g/dl); TP, total protein (g/dl). (n = 6–8 mice/group). ± SEM; *$p < 0.05$

or vehicle control groups with the exception of neutrophil (NEU) and red blood cell (RBC) counts, which were significantly higher in the ALW-II-41-27 treated group, but still within normal published parameters [15]. These mild elevations were not clinically significant. While the mechanisms for these slight increases are unknown, one

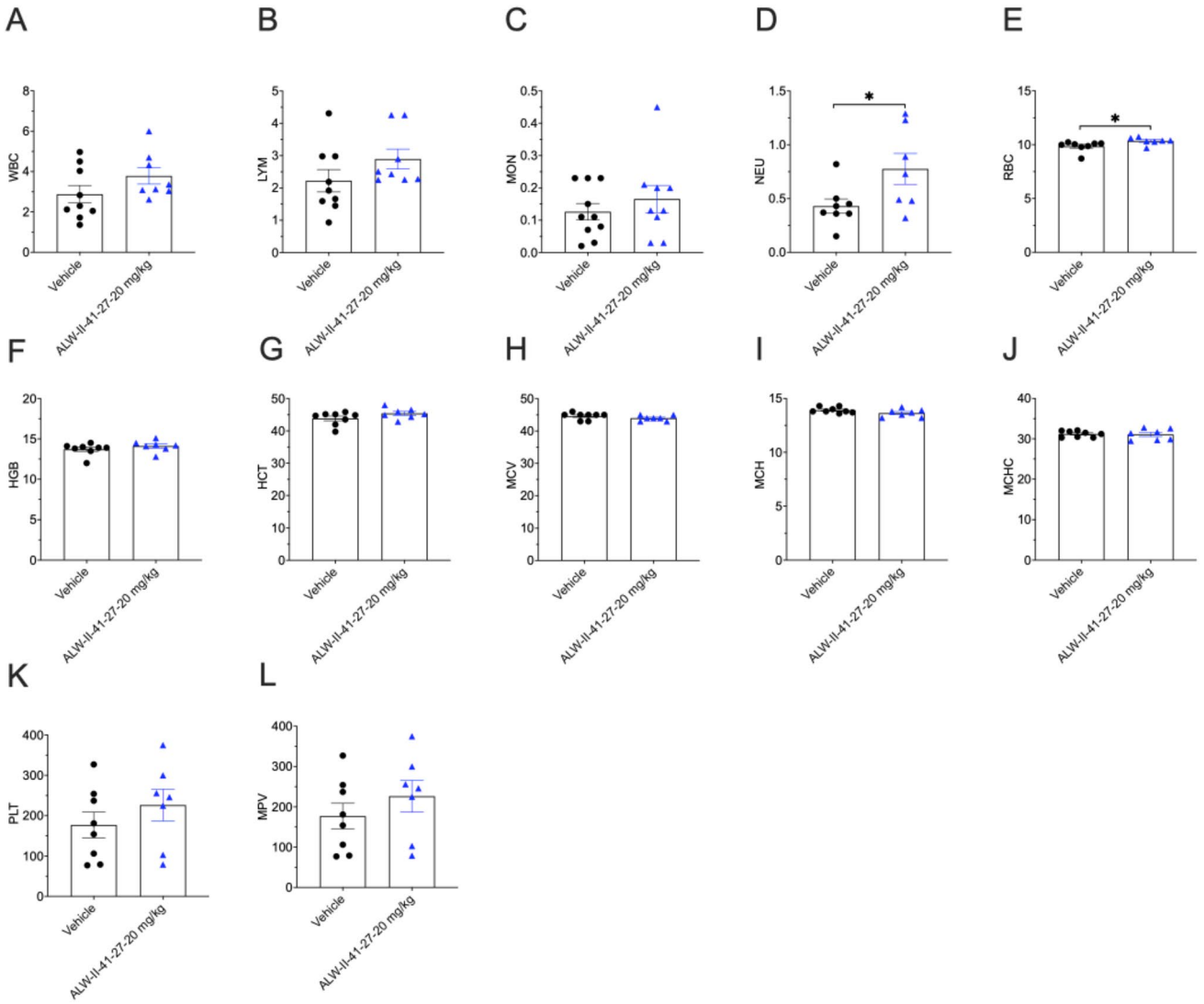

Fig. 6 CBC analysis. WBC, total white blood cells (10^9/l); LYM, lymphocytes (10^9/l); MON, monocytes (10^9/l); NEU, neutrophils (10^9/l); RBC, red blood cells (10^{12}/l); HGB, hemoglobin (g/dl); HCT, hematocrit (%); MCV, mean corpuscular volume (fL); MCH, mean corpuscular hemoglobin (pg); MCHC, mean corpuscular hemoglobin concentration (g/dl); PLT, platelets (10^9/l); MPV, mean platelet volume (fL). ($n = 7$–8 mice/group). ± SEM; *$p < 0.05$

might posit that ALW-II-41-27 may increase the release of these blood cells from the bone marrow.

3.7 Histology analysis

Histologic examination of all samples from lung, liver, and kidney from both ALW-II-41-27 treated and vehicle groups did not reveal any toxic abnormalities and all organs displayed normal architecture (Fig. 7) (score of 0 for all parameters).

3.8 In Vivo ALW-II-41-27 Anti-inflammatory Analysis

Analysis of the effects of two doses of ALW-II-41-27 intraperitoneal the day before (18 h) and 2 h before the intratracheal injection of yeast β-glucans demonstrated significant decreases in IL-1β in lung protein lysates as measured by ELISA, indicating in vivo activity of the ALW-II-41-27 on fungal induced lung inflammation (Fig. 8).

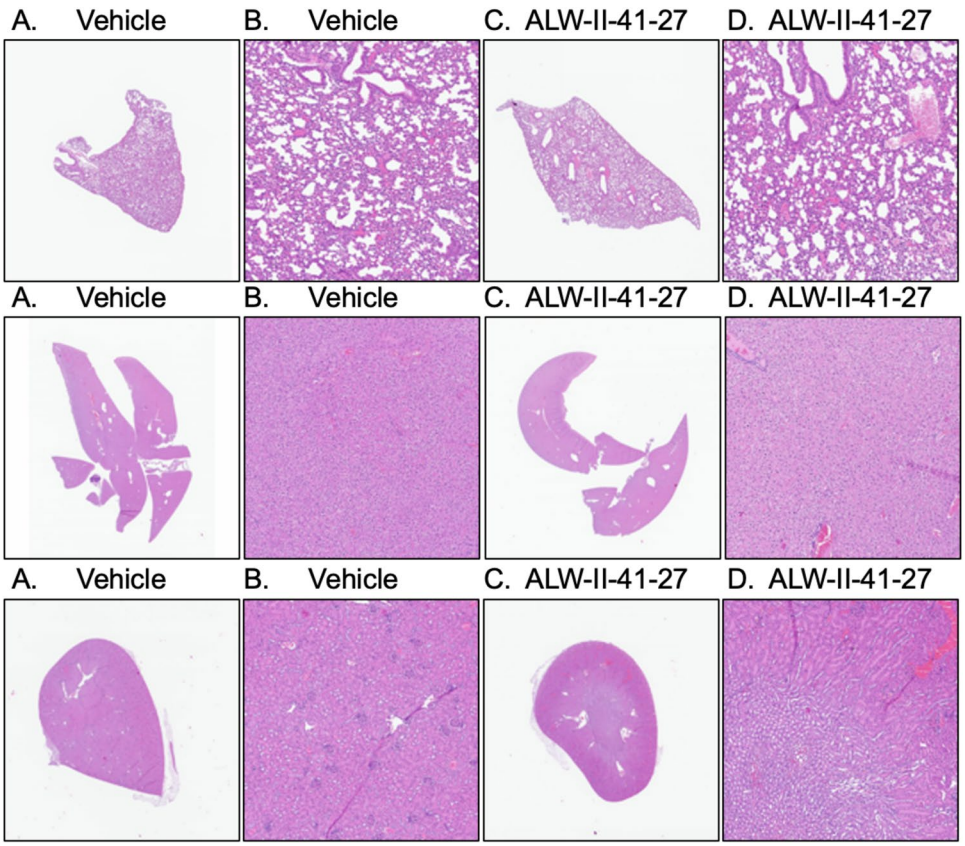

Fig. 7 Lung, liver, and kidney histopathology of 10-day IP-treated vehicle or ALW-II-41-27 EphA2 inhibitor. Hematoxylin and eosin (H&E) staining was performed on sections of lung (top panels), liver (middle panels), and kidney (bottom panels) from mice in all groups. **A**, **B** Vehicle control. **C**, **D** ALW-II-41-27 at 20.0 mg/kg. **A**, **C** × 1 magnification. **B**, **D** × 10 magnification. No gross histological changes were present in lung, liver, or kidneys in the vehicle or ALW-II-41-27 inhibitor administration

4 Discussion

Fungi are major contributors in opportunistic infections in those with advanced human immunodeficiency virus (HIV). *Pneumocystis* pneumonia (PCP), caused by *Pneumocystis jirovecii* is a common pathogen in acquired immunodeficiency syndrome (AIDS) populations across the globe. Implementation of highly active antiretroviral therapy (HAART) has decreased the overall incidence of PCP, but the ability to receive this treatment is limited and cases requiring hospitalization and associated mortality remains quite high [16].

The current anti-*Pneumocystis* therapy based on trimethoprim–sulfamethoxazole (TMP–SMX) has proven to an effective antimicrobial combination to treat *Pneumocystis jirovecii* pneumonia (PJP). Although effective, the host inflammatory response following fungal cell death during treatment, through the exposure of newly exposed β-glucans can prove highly detrimental to the host [17–19]. Indeed, when corticosteroids are utilized in patients with HIV with moderate–severe PJP, there is a significant decrease in mortality and morbidity [20]. In patients without HIV, data on adjuvant corticosteroids is less clear and no consensus has yet been determined. Even though steroids may be beneficial to the patient in these settings, there are still both short-term (co-infections, hyperglycemia) and long term (myopathy and osteoporosis) side effects that need to be considered [21].

Anti-inflammatory therapy in general, in the setting of infectious diseases, is not universally advantageous and is not yet established in many infectious diseases. Depending on the infection, cytokine-driven inflammatory responses may be required for effective elimination of infection. However, in the case of *Pneumocystis* pneumonia, anti-inflammatory corticosteroids have been shown beneficial and are routinely administered to patients with moderately severe disease [22]. Such treatment reduces the risk of respiratory failure and death during PCP [20].

Accordingly, we believe that other adjunct therapies should be developed for PJP. Recently, we have demonstrated that macrophages pre-incubated in vivo with the EphA2 receptor inhibitor ALW-II-41-27 have significant reductions in their ability to generate proinflammatory signaling and downstream TNFα production following stimulation with *Pneumocystis* β-glucans [9]. Other have shown that the Ephrin receptor EphB2 can bind fungal β-glucans and in collaboration with Dectin-1 can activate the Dectin-1 signaling pathway [23]. ALW-11-41-27 has also been shown to inhibit this receptor as well, but its roles in inhibiting the EphB2/Dectin-1 signaling cascade is unknown [24]. These results led us to hypothesize that ALW-II-41-27 may be used in vivo as an adjunct therapy similar to corticosteroids [9]. As

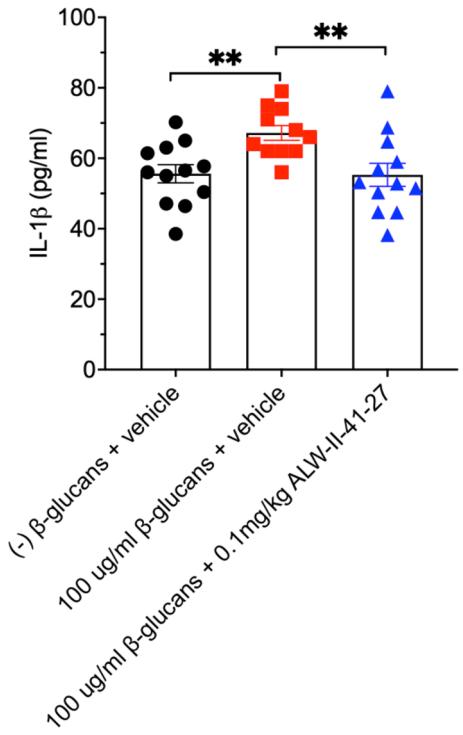

Fig. 8 Effects of IP injection of ALW-II-41-27 on yeast β-glucan-induced proinflammatory response. 20 h prior to giving mice 100 µg/ml *Saccharomyces cerevisiae* β-glucans via IT injection, mice were given 0.1 mg/kg ALW-II-41-27 or the vehicle control via IP as noted above. The next day at 18 h post ALW-II-41-27 or vehicle treatment, mice were given another 0.1 mg/kg of ALW-II-41-27, or vehicle as stated. After 2 h, mice were given ± 100 µg/ml *S. cerevisiae* β-glucans via IT. The following day mice were sacrificed, and lung protein lysates (50 µg total) measured for IL-1β. Bar graph represents the results from 11 to 12 mice per group. ± SEM; **$p < 0.01$

part of the development toward human clinical application, a thorough preclinical assessment was required to evaluate the safety and potential toxicities of the ALW-II-41-27 EphA2 inhibitor. To the best of our knowledge, this is the first in-depth study reported to examine this. The preclinical data presented here supports that ALW-II-41-27 is a viable anti-inflammatory therapeutic approach that is appropriate for further preclinical development.

In this study, we dosed mice ALW-II-41-27 at 20.0 mg/kg once a day for 11 days via IP administration based on the preliminary PK data. The administration of ALW-II-41-27 appeared to be well tolerated in mice at the tested doses. Parameters such as weight loss, lung-specific proinflammatory response, lung extracellular matrix mRNA generation, blood chemistry, and CBC analysis, and H&E histological examination of lung, liver, and kidney samples demonstrated no significant changes compared to the vehicle control. Furthermore, we demonstrated that treatment of mice with the EphA2 inhibitor ALW-II-41-27 prior to the addition of fungal β-glucans, a major cell wall proinflammatory constituent of pathogenic fungi, including *Pneumocystis*, also significantly reduced IL-1β production in the lung tissue, supporting its further development as an anti-inflammatory agent.

5 Conclusions

Based on these findings, the use of ALW-II-41-27 EphA2 inhibitor appears safe and can be used to reduce the deleterious effects of the host inflammation in further investigations of the murine PCP model and potentially other models of lung inflammation.

Supplementary Information The online version contains supplementary material available at https://doi.org/10.1007/s40268-024-00483-5.

Declarations

Funding This work was supported by the Mayo Foundation; the Walter and Leonore Annenberg Foundation, and NIH grants R21AI181542-01 and R01 HL62150-30A1 to A.H.L.

Conflict of interest The authors declare no conflict of interest.

Ethics approval This study was approved by the Mayo Clinic Institutional Animal Care and Use Committee (IACUC) approved protocol A00007116-23 on 9/5/2023.

Consent to participate Not applicable.

Consent for publication Not applicable

Availability of data and material The datasets generated and/or analyzed during the current study are available from the corresponding author on reasonable request.

Code availability Not applicable.

Author contributions T.J.K., K.E.S., M.R.P., M.B., E.S.Y., and A.H.L. made substantial contributions to the conception or design of the work, or the acquisition, analysis, or interpretation of data. All authors approved the version to be published.

References

1. de Boer ECW, van Gils JM, van Gils MJ. Ephrin-Eph signaling usage by a variety of viruses. Pharmacol Res. 2020;159: 105038.
2. Su C, et al. Molecular basis of EphA2 recognition by gHgL from gammaherpesviruses. Nat Commun. 2020;11(1):5964.
3. Swidergall M, et al. Activation of EphA2-EGFR signaling in oral epithelial cells by *Candida albicans* virulence factors. PLoS Pathog. 2021;17(1): e1009221.
4. Swidergall M, et al. EphA2 is a neutrophil receptor for *Candida albicans* that stimulates antifungal activity during oropharyngeal infection. Cell Rep. 2019;28(2):423–33 (**e5**).
5. Zhang J, et al. MiR-26a targets EphA2 to resist intracellular Listeria monocytogenes in macrophages. Mol Immunol. 2020;128:69–78.
6. Swidergall M, et al. Publisher Correction: EphA2 is an epithelial cell pattern recognition receptor for fungal beta-glucans. Nat Microbiol. 2018;3(3):387.
7. Kottom TJ, et al. EphA2 Is a lung epithelial cell receptor for pneumocystis beta-glucans. J Infect Dis. 2022;225(3):525–30.
8. Kottom TJ, Carmona EM, Limper AH. Targeting host tyrosine kinase receptor EphA2 signaling via small-molecule ALW-II-41-27 inhibits macrophage pro-inflammatory signaling responses to *Pneumocystis carinii* beta-glucans. Antimicrob Agents Chemother. 2024;68(2): e0081123.
9. Kottom TJ, Carmona EM, Limper AH. Targeting CARD9 with small-molecule therapeutics inhibits innate immune signaling and inflammatory response to *Pneumocystis carinii* beta-glucans. Antimicrob Agents Chemother. 2020. https://doi.org/10.1128/AAC.01210-20.
10. Rennard SI, et al. Estimation of volume of epithelial lining fluid recovered by lavage using urea as marker of dilution. J Appl Physiol. 1986;60(2):532–8.
11. Kottom TJ, et al. Preclinical and toxicology studies of BRD5529, a selective inhibitor of CARD9. Drugs R D. 2022;22(2):165–73.
12. Choudhury M, et al. Targeting pulmonary fibrosis by SLC1A5-dependent glutamine transport blockade. Am J Respir Cell Mol Biol. 2023;69(4):441–55.
13. Kang JH, et al. Transforming growth factor beta induces fibroblasts to express and release the immunomodulatory protein PD-L1 into extracellular vesicles. FASEB J. 2020;34(2):2213–26.
14. Meneton P, et al. Renal physiology of the mouse. Am J Physiol Renal Physiol. 2000;278(3):F339–51.
15. Nemzek JA, et al. Differences in normal values for murine white blood cell counts and other hematological parameters based on sampling site. Inflamm Res. 2001;50(10):523–7.
16. Thomas CF Jr, Limper AH. Current insights into the biology and pathogenesis of Pneumocystis pneumonia. Nat Rev Microbiol. 2007;5(4):298–308.
17. Evans HM, et al. The trophic life cycle stage of the opportunistic fungal pathogen *Pneumocystis murina* hinders the ability of dendritic cells to stimulate CD4(+) t cell responses. Infect Immun. 2017. https://doi.org/10.1128/IAI.00396-17.
18. Kutty G, et al. beta-Glucans are masked but contribute to pulmonary inflammation during Pneumocystis pneumonia. J Infect Dis. 2016;214(5):782–91.
19. Linke MJ, et al. Characterization of a distinct host response profile to Pneumocystis murina asci during clearance of pneumocystis pneumonia. Infect Immun. 2013;81(3):984–95.
20. Bozzette SA, et al. A controlled trial of early adjunctive treatment with corticosteroids for *Pneumocystis carinii* pneumonia in the acquired immunodeficiency syndrome. California Collaborative Treatment Group. N Engl J Med. 1990;323(21):1451–7.
21. Weyant RB et al. *Pneumocystis jirovecii*: a review with a focus on prevention and treatment. Expert Opin Pharmacother 2021; 1–14.
22. Limper AH, et al. An official American Thoracic Society statement: treatment of fungal infections in adult pulmonary and critical care patients. Am J Respir Crit Care Med. 2011;183(1):96–128.
23. Sun W, et al. Cutting edge: EPHB2 is a coreceptor for fungal recognition and phosphorylation of SYK in the dectin-1 signaling pathway. J Immunol. 2021;206(7):1419–23.
24. Zhang L, et al. EphrinB2/ephB2-mediated myenteric synaptic plasticity: mechanisms underlying the persistent muscle hypercontractility and pain in postinfectious IBS. FASEB J. 2019;33(12):13644–59.